Journal of ELECTRONIC MATERIALS, Vol. 46, No. 1, 2017
DOI: 10.1007/s11664-016-4900-z

Ni/Pd-Decorated Carbon NFs as an Efficient Electrocatalyst for Methanol Oxidation in Alkaline Medium

IBRAHIM M.A. MOHAMED,[1] KHALIL ABDELRAZEK KHALIL,[2,3] HAMOUDA M. MOUSA,[1,5] and NASSER A.M. BARAKAT[1,4,6]

1.—Bionanosystem Engineering Department, Chonbuk National University, Jeonju 561-756, Republic of Korea. 2.—Mechanical Engineering Department, King Saud University, P.O. Box 800, Riyadh 11421, Saudi Arabia. 3.—Materials Engineering and Design Department, Aswan University, Aswan, Egypt. 4.—Chemical Engineering Department, Faculty of Engineering, Minia University, El-Minia, Egypt. 5.—Department of Engineering Materials and Mechanical Design, Faculty of Engineering, South Valley University, Qena 83523, Egypt. 6.—e-mail: nasser@jbnu.ac.kr

In this study, Ni/Pd-decorated carbon nanofibers (NFs) were fabricated as an electrocatalyst for methanol oxidation. These NFs were synthesized based on carbonization of poly(vinyl alcohol), which has high carbon content compared to many polymers used to prepare carbon NFs. Typically, calcination of an electrospun mat composed of nickel acetate, palladium acetate, and poly(vinyl alcohol) can produce Ni/Pd-doped carbon NFs. The introduced NFs were characterized by scanning electron microscopy, transmission electron microscopy (TEM), high-resolution transmission electron microscopy, line TEM energy dispersive x-ray spectrometry, field emission scanning electron microscopy, and x-ray powder diffraction. These physicochemical characterizations are acceptable tools to investigate the crystallinity and chemistry of the fabricated Ni/Pd-carbon NFs. Accordingly, the prepared NFs were tested to enhance the economic and catalytic behavior of methanol electrooxidation. Experimentally, the obtained onset potential was small compared to many reported materials; 0.32 V (versus Ag/AgCl as a reference electrode). At the same time, the current density changed from 5.08 mA/cm^2 in free methanol at 0.6 V to 12.68 mA/cm^2 in 0.1 mol/L methanol, which can be attributed to the MeOH oxidation. Compared to nanoparticles, the NFs have a distinct effect on the electrocatalytic performance of material due to the effect of the one-dimensional structure, which facilitates the electron transfer. Overall, the presented work opens a new way for non-precious one-dimensional nanostructured catalysts for direct methanol fuel cell technology.

Key words: Electrospinning, methanol electrooxidation, nanofibers, Ni/Pd, fuel cell

INTRODUCTION

Nowadays, direct methanol fuel cells (DMFCs) have received much attention,[1–6] because methanol is non-precious, available, and an easily transported fuel. Furthermore, the reaction rate of methanol oxidation is high because the chemical structure doesn't contain a carbon-carbon (C-C) bond, and finally its energy density is 6100 W h kg^{-1}.[7,8] The commercialization of DMFCs is quite dependent on the cost, activity, and durability of the electrocatalyst. At present, almost all low-temperature fuel cells use Pt-based electrocatalysts. Accordingly, the manufacturing cost is relatively high, which reduces their wide applications.[3,9,10]

In DMFCs, methanol is oxidized to carbon dioxide according to the reaction: $CH_3OH + H_2O = CO_2$

(Received November 10, 2015; accepted August 19, 2016; published online September 12, 2016)

$+6H^+ + 6e$. This reaction has two steps: adsorption and electrochemical reaction on the anode surface.[11] Accordingly, carbon materials have high adsorption capacity, so they were used to enhance the electrocatalytic performance for many electrodes.[12]

NFs have gained much significance because of the heightened awareness of their potential applications in many fields, including medicine, engineering, and chemical synthesis. Electrospinning is a simple, effective, and non-precious technique to synthesize NFs. Moreover, it is easy to dominate the morphology, chemical and pore structure of the produced NFs.[13,14] Compared to nanoparticles, the large axial ratio gives the nanofiber catalysts a distinct merit, especially when used in the electron transfer-based processes.[15] Certainly, carbon NFs are widely used in many fields such as dye-sensitized solar cells,[16,17] high performance supercapacitor,[18] non-enzymatic glucose detection,[19] capacitive deionization,[20] lithium-ion rechargeable batteries,[21] and direct methanol fuel cells.[22,23] Based on chemical content, poly(vinyl alcohol) (PVA) has a high carbon content (ca.54.5%) and contains hydroxyl groups in the polymer chain, which makes it favorable for the production of carbon NFs after calcination. However, decomposition of PVA before carbonization is the main problem for the known low yield. Recently, it was reported that transition metals can be used as effective catalysts for PVA carbonization and consequently strongly enhance the yield.[24]

Ni and Pd have similar chemical properties to Pt, which is the most widely used as anode catalyst in DMFCs, because these elements are in the same group in the periodic table. Ni is used to increase the performance and durability of Pt.[1,25,26] Ni-N carbon NFs have a good electroactivity in methanol oxidation.[27] Pd and Pd/C catalysts can control the poisoning of CO.[28] Thus, Ni/Pd carbon NFs are a promising non-precious electrocatalyst in direct methanol fuel cells.

The target of this work is fabrication of novel cheap materials with high electrocatalytic activity toward methanol electrooxidation. Accordingly, enhancement of the electrocatalytic activity will be based on exploiting the influence of synergetic effect of nickel and palladium bimetallic nanoparticles, as well as the merit of the nanofibrous morphology. At last, Ni/Pd-decorated carbon NFs were prepared and tested as an efficient catalyst for methanol electrooxidation.

EXPERIMENTAL

Materials

Poly(vinyl alcohol) (PVA) (M.wt = 65,000 g/mol, DC Chemical Co., South Korea), nickel acetate tetra hydrate (NiAc, 98.0% assay, Sigma-Aldrich), palladium acetate (PdAc 98% assay, Sigma-Aldrich), potassium hydroxide (KOH 99% assay, Sigma-Aldrich) were used without any further modifications. De-ionized water was used as a solvent all over this work.

Synthesis of Ni/Pd Carbon NFs (CNFs)

At first, a sol–gel is prepared by dissolving 0.9 g of NiAc and 0.1 g of PdAc in 3 mL de-ionized water followed by addition of poly(vinyl alcohol) aqueous solution (10%). The percentage of polymer in sol–gel is 8.33%. Secondly, the mixture was stirred at 50°C for 3 h. Then, the obtained viscous solution was electrospun at 18 kV to produce NFs. The distance between negative electrode (rotating cylinder) and positive electrode (needle tip) was adjusted to be 20 cm. At last, drying the obtained NFs was carried out at 70°C for 48 h under vacuum. The NFs were carbonized under vacuum at 900°C for 2 h with a heating rate of 2°C.

Characterization of Ni/Pd Carbon Nanofiber

The microstructure and morphology were investigated by scanning electron microscope (SEM) (JEOL JSM 7100F, Japan) and field emission scanning electron microscope (FE-SEM) (JEOL-JSM- 2100F, Japan). The crystallinity of the fiber was demonstrated by x-ray diffractometer (XRD, Rigaku, Japan) with Cu-Kα (λ = 1.54056 Å) radiation over Braggangle 2θ ranging from 5° to 100°. The rate of scanning is 5°/min. The mapping of Ni, Pd, and carbon is demonstrated by transmission electron microscopy (TEM). TEM was measured by JEOL JEM-2200FS TEM at 200 kV (JEOL, Japan).

Preparation of Working Electrode

Two milligrams of Ni/Pd carbon NFs were sonicated in a mixture of 400 μL of 2-propanol and 20 μL of Nafion solution to form suspension. The glassy carbon electrode was polished and washed by ethanol and acetone. The electrode was coated by 15 μL of catalyst. Then the electrode dried under air for 40 min at 70°C.[29] The weight of active catalyst in electrode surface is 0.071 mg.

Electrochemical Measurements

The electrocatalytic activity of the introduced Ni/Pd-doped carbon NFs was studied by cyclic voltammetry technique. The cyclic voltammetry measurements were carried out in 1 mol/L KOH at 298 K and measured by VersaSTAT 4, USA. Ag/AgCl was used as a reference electrode, Pt wire was used as an auxiliary electrode. Chronoamperometric technique was exploited to study the stability of the studied catalyst at 0.4 V and 298 K.

RESULTS AND DISCUSSION

Fabrication of Ni/Pd Decorated Carbon NFs

In this work, we used a simple and effective technique: electrospinning. A high voltage is applied to obtain fine polymer NFs.[15] The studied NFs are

prepared using metal acetate of Ni and Pd in the presence of poly vinyl alcohol. Metal acetate has a good poly condensation characters as displayed in Scheme 1,[30] which leads to the formation of electrospun carbon NFs with good morphology. Accordingly, metal acetates are the most widely used inorganic precursor for fabrication of metallic NFs using the electrospinning process.[15]

In fact, the prepared material has a good nanofibrous morphology as seen in Fig. 1. The material was investigated at high magnification (Fig. 1a), low magnification (Fig. 1b), and after carbonization (Fig. 1c and d). Experimentally, calcination of the obtained electrospun fiber mat under vacuum doesn't deeply affect the nanofibrous morphology as shown in Fig. 1c and d. Figure 2 describes the FESEM image of the prepared catalyst: it is shown that nanoparticles are incorporated in the obtained NFs after calcination. Figure 3a shows the TEM image which vouches the formation of the metallic nanoparticles in carbon NFs. High resolution transmission electron microscope is studied to investigate the internal structure of the NFs as shown in Fig. 3b. This figure shows the metallic content (yellow squares) and non-metallic content (blue circles), which is due to carbon NFs. Figure 3c shows the mapping of carbon, nickel, and palladium. From this mapping, it can be concluded that the investigated catalyst contains Ni/Pd and covered by carbon NFs. Also, Ni has the highest concentration in this sample. To get more information about the chemical content of the studied catalyst, Line TEM EDX analyses were carried out; Fig. 4. It is easy to see that the sample contain mainly Ni and C with small portion from Pd. To conclude, the morphology and chemistry of the prepared material is Ni/Pd nanoparticles decorated carbon NFs.

Among the different physical techniques, XRD has the confidence to find information about the crystallinity and chemistry of the prepared material, especially the formation of metal nanoparticles. Figure 5 presents the XRD pattern of the carbonized Ni/Pd carbon NFs. The broad peak around 26.4 corresponding to (002) plane of the graphite-like structure. The other strong peaks at 43.08, 50.19, and 73.59 agree with crystal planes (111),

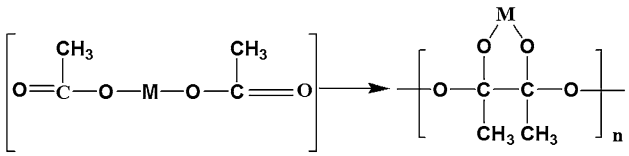

Scheme 1. Poly condensation of the metal acetate precursors; M can be Ni or Pd.

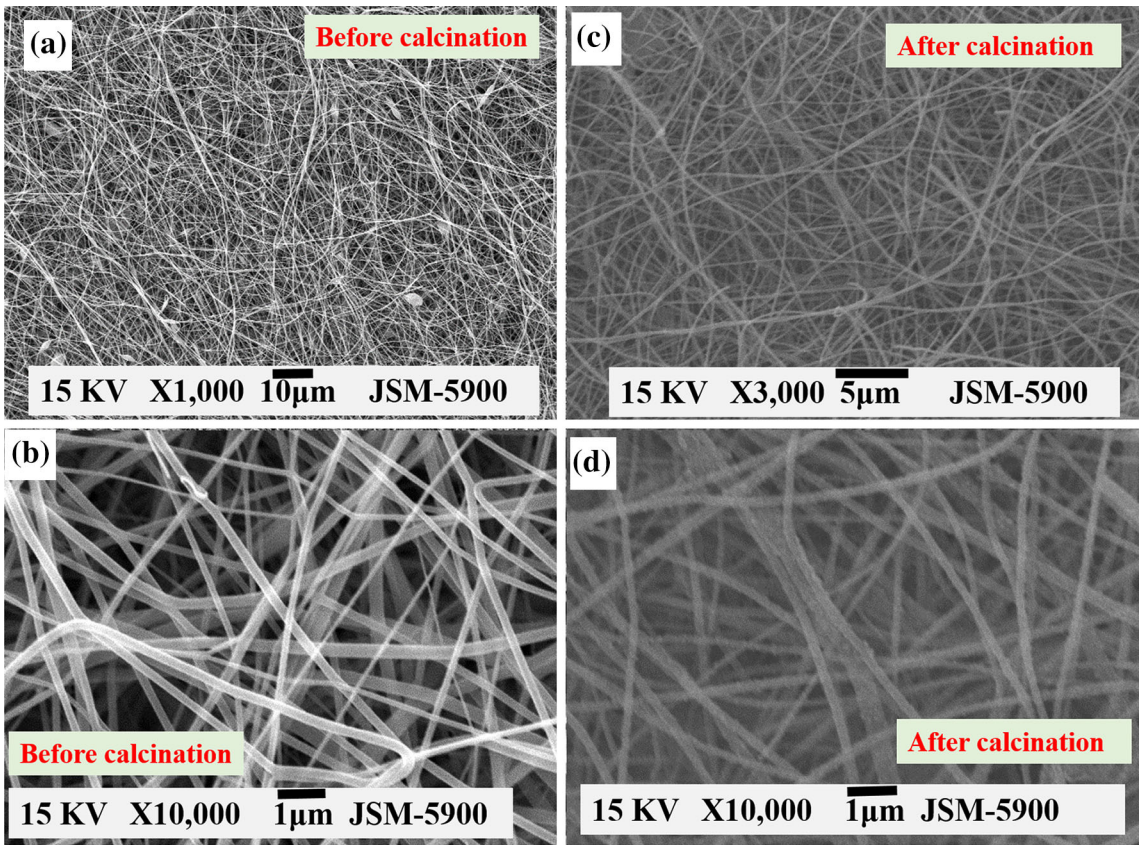

Fig. 1. Low and high magnifications SEM images for the prepared material before (a and b) and after (c and d) calcination.

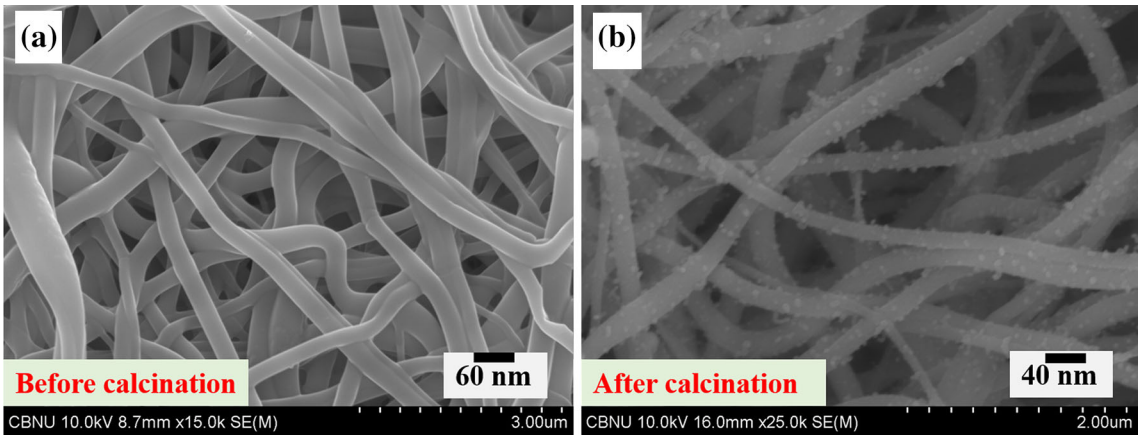

Fig. 2. FESEM images of the investigated nanofibers before (a) and after (b) calcination.

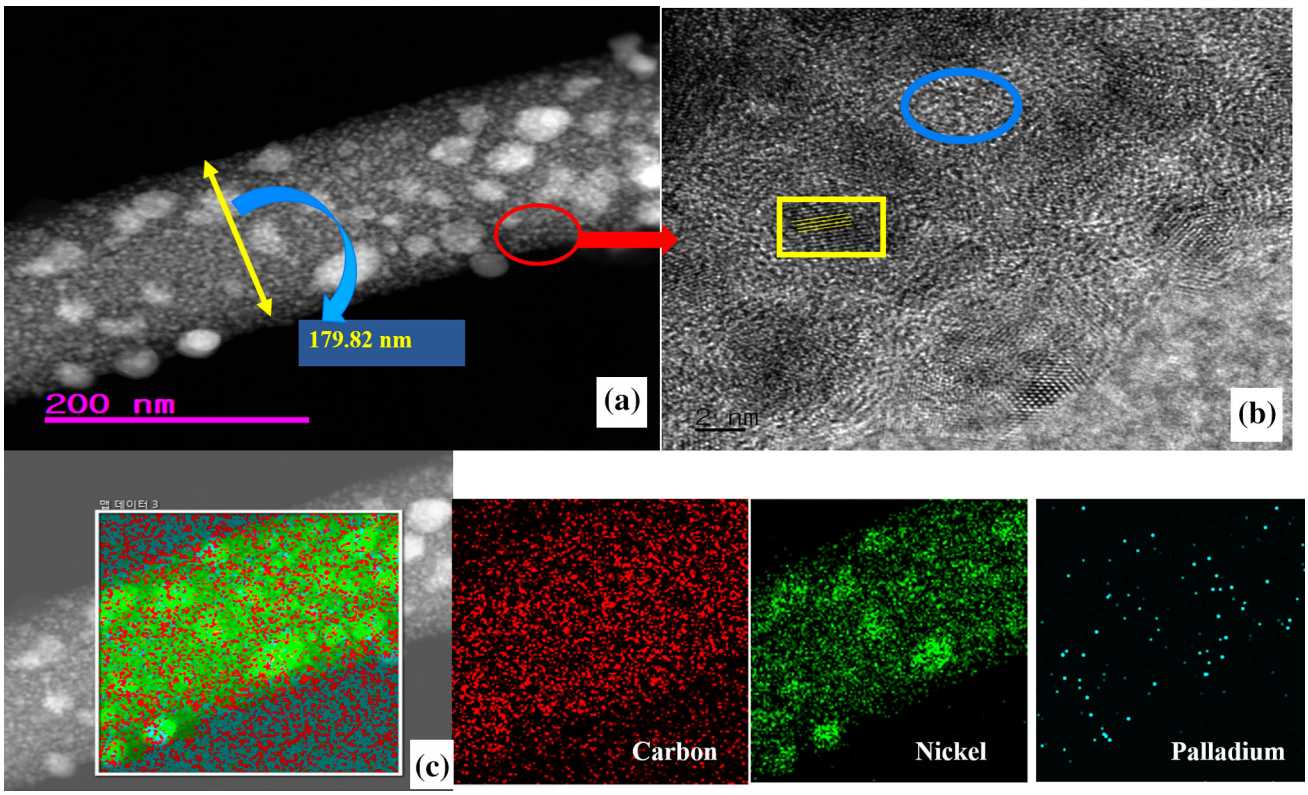

Fig. 3. TEM image (a), HR-TEM image (b), and elemental mapping (c) for the sintered nanofibers. The blue circle in panel B refers to the non-metallic content (carbon) and the yellow square points to the metallic content (Ni/Pd) (Color figure online).

(200), and (220) of Ni with some shift in the position of each reflection peak if compared to Ni pure (JCDPS# 04-0850). This shift is due to the presence of Pd, as reported by Zhao et al.[31] Because of the small amount of used Pd precursor compared to Ni, the detected peaks of Pd revealed low intensity as shown in the figure; however, the marked peaks in the pattern matches the standard Pd peaks based on the XRD database (JCDPS# 46-1043).

The decomposition of acetate in the absence of air produces hydrogen and carbon monoxide gases which can act as reducing agents; as such, these gases may help to obtain pure metal without any oxide.[32] Scheme 2 explains the production of pure Ni from nickel acetate under high temperature.[33] It is noteworthy to mention that Pd has lower chemical activity than Ni, so it is expected to decompose more easily than Ni.

Figure 6 displays the thermal gravimetric analysis (TGA) of the original NiAc/Pd/PVA electrospun NFs under argon atmosphere. As shown, the weight starts to decrease slowly in the beginning due to

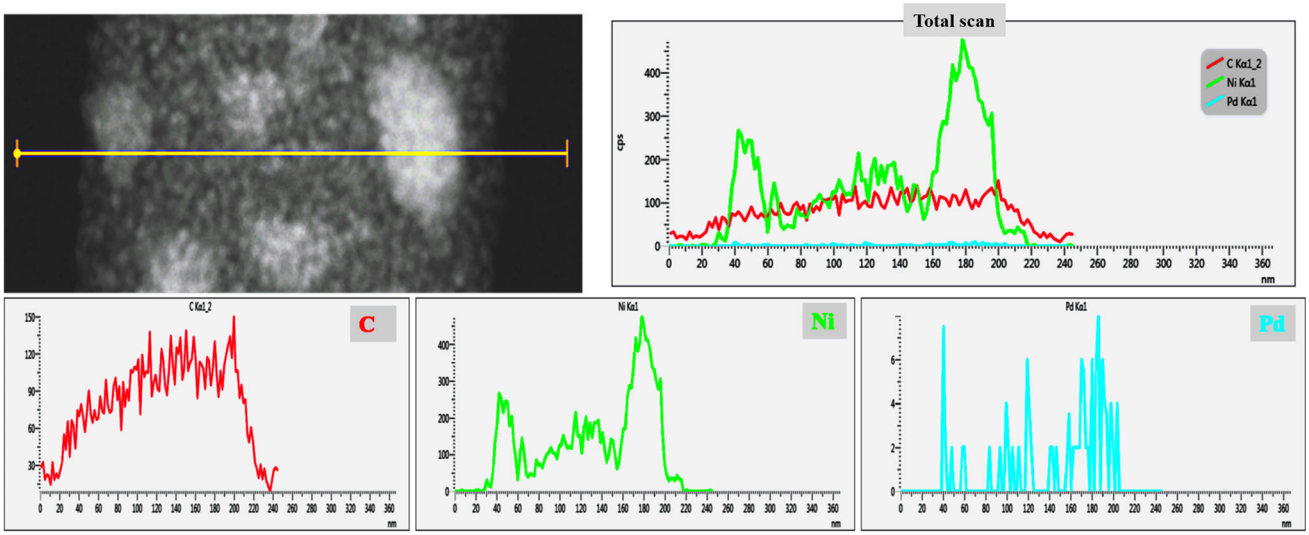

Fig. 4. Line TEM EDX analysis results for the introduced Ni/Pd NPs-doped carbon nanofibers at random chosen line.

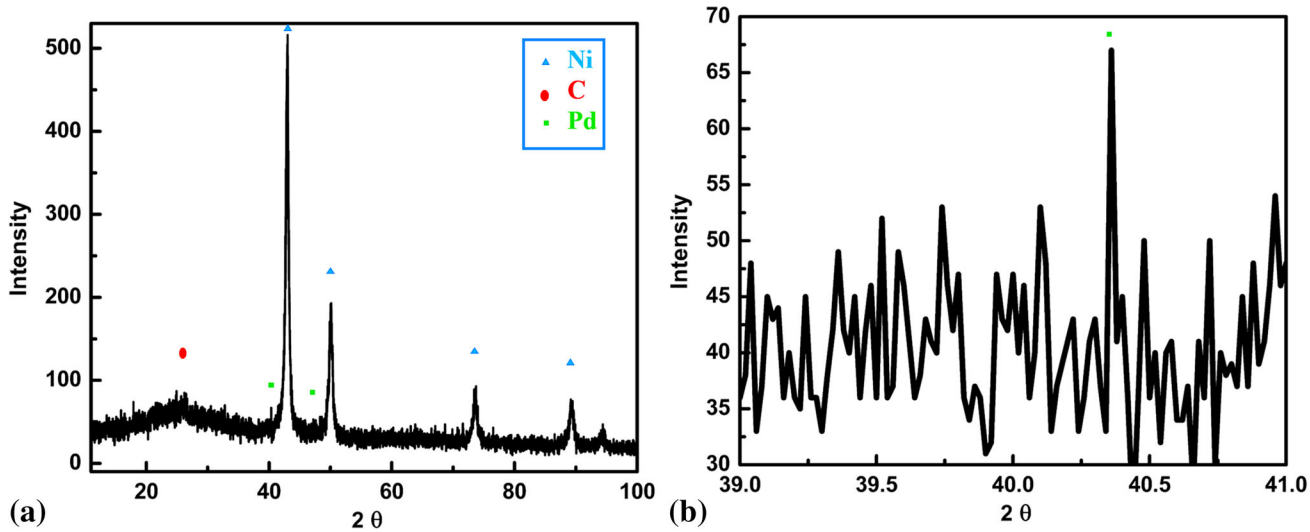

Fig. 5. XRD pattern of the prepared Ni/Pd–doped carbon nanofibers (a) and high magnification in the 2θ range of (38–41) (b).

$$Ni(CH_3COO).4H_2O \longrightarrow 0.86\ Ni(CH_3COO)_2.0.14\ Ni(OH)_2 + 0.28\ CH_3COOH + 3.72\ H_2O \quad (1)$$

$$0.86\ Ni(CH_3COO)_2.0.14\ Ni(OH)_2 \longrightarrow NiCO_3 + NiO + CH_3COCH_3 + H_2O \quad (2)$$

$$NiCO_3 \longrightarrow NiO + CO_2 \quad (3)$$

$$NiO + CO \longrightarrow Ni + CO_2 \quad (4)$$

Scheme 2. Decomposition of nickel acetate under inert atmosphere at high temperature.

evaporation of the physical water content (moisture). Later on, a sharp decrease in the weight can be observed, which is attributed to decomposition of the metallic precursor and graphitization of the polymer. Finally, a constant weight can be seen after the temperature reaches 720°C. Based on

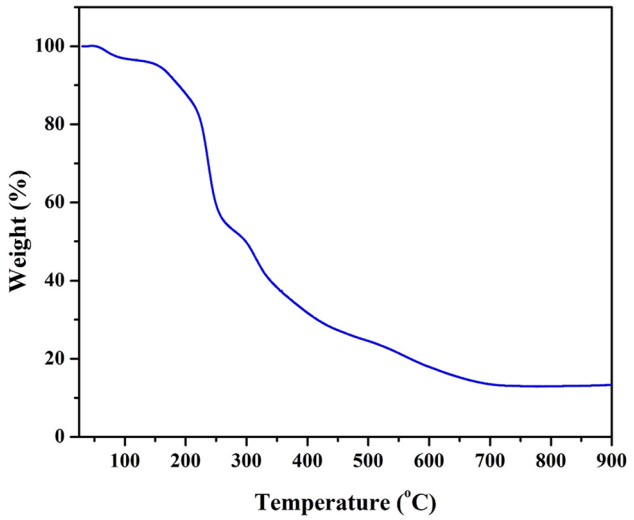

Fig. 6. Thermal gravimetric analysis for the electrospun NiAc/Pd/PVA nanofibers in argon atmosphere.

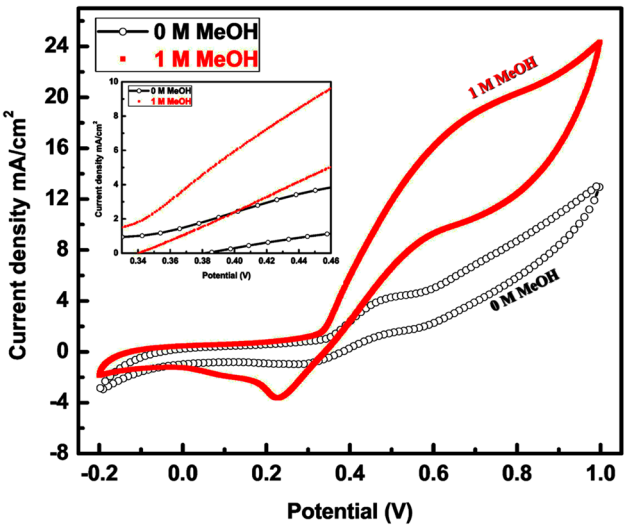

Fig. 7. Cyclic voltammetry of Ni/Pd-doped CNFs in 1 M KOH with and without methanol addition at a scan rate of 50 mV/s and 25°C using Ag/AgCl as a reference electrode. The inset displays high magnification at the onset potential window.

Scheme 2 and also other studies,[34] the metal precursor (nickel acetate) will be converted to pristine nickel nanoparticle. Considering that Ni and Pd have melting points (1485°C and 1585°C, respectively) higher that the calcination temperature, it is difficult to expect losing any metal content. Therefore, from the remaining weight (13 wt.%), carbon content in the final NFs can be determined to be 5.7 wt.%. Accordingly, Ni/Pd NPs represent 94.3 wt.%.

Electrochemical Study of Ni/Pd-Doped Carbon NFs

Scientifically, the best tool to investigate oxidation is cyclic voltammetry. Figure 7 shows the cyclic voltammetry of the prepared Ni/Pd decorated carbon NFs as a working electrode in an alkaline medium with and without methanol to study the catalytic activity of this material for methanol electrooxidation. As shown in the figure, the Ni/Pd-carbon NFs can be considered as an efficient electrocatalyst for methanol oxidation in alkaline medium. Experimentally, the current density increased from 4.17 mA/cm^2 to 11.31 mA/cm^2 at the same potential 0.48 mV versus Ag/AgCl as a reference electrode. This performance can be attributed to two things: (a) nanofibrous morphology, which facilitates the electron transfer-based reactions, and (b) presence of vacant orbitals of transition metals (Ni and Pd), which can act as an active sites for electrons of oxygen.[35] Moreover, the presence of Pd, which has high electrocatalytic activity in alkaline fuel cells,[36,37] may form bifunctional effects with Ni.

In contrast to Pt, the zero valent surface of the transition metals first row cannot be used for the electrocatalytic activity without pre-activation. In the alkaline medium, Ni reacts with hydroxide group to form nickel hydroxide ($Ni(OH)_2$) which can increase the electroactivity. Typically, in the voltammogram of the pristine nickel, usually two regions are observed; the first region is in the negative potential side comprising a small anodic peak the oxidation of nickel according to the reaction[38]:

$$Ni + 2OH^- \rightleftarrows Ni(OH)_2 + 2e$$

Then, $Ni(OH)_2$ may be oxidized to NiOOH in accordance with this reaction[39,40]:

$$Ni(OH)_2 + OH^- \rightleftarrows Ni(OOH) + H_2O + e$$

Based on many reports about electrocatalytic activity of Ni nanoparticles in alkaline medium, Ni(OOH) can play an important role for the Ni electrocatalytic activity. Experimentally, the prepared NFs have activation peaks in alkaline medium as shown in Fig. 8 which can be attributed to the formation of a Ni(OOH) layer. These redox peaks increased with increasing cycle number until an activation process will be completed. Increasing the number of potential sweeps results in a progressive increase of the current density values of the cathodic peak (Fig. 8) because of the entry of OH^- into the $Ni(OH)_2$ surface layer, which leads to the progressive formation of a thicker NiOOH layer corresponding to the $Ni(OH)_2$/NiOOH transition.[38]

The efficiency of direct methanol fuel cell was affected by methanol concentration. The maximum power density changed to 20 mW/cm^2 from 10.7 mW/cm^2, when the concentration of methanol increased from 1 mol/L to 5 mol/L using Pt/Ru as a catalyst.[41] Thus, the effect of methanol concentration on the electrocatalytic activity of the introduced Ni/Pd-doped carbon NFs was studied; the results

are shown in Fig. 9. As the methanol concentration increased, the current density increased, which indicates oxidation of methanol molecules on the surface of the synthesized NFs. Another finding that can be observed is the optimum methanol concentration of 5 M, which is high if compared to many reported electrocatalysts. The onset potential is an important indicator among the invoked parameters to demonstrate the electrocatalytic activity. The onset potential indicates the electrode overpotential. In alcohol electrooxidation, lower onset potential indicates high activity. As shown in the obtained results (Fig. 9a), the corresponding onset potential of the introduced NFs is ~320 mV (versus Ag/AgCl). This finding further supports the electrocatalytic efficiency of the studied NFs. Figure 9b shows the effect of methanol concentration in maximum current density at four potentials 0.5 V, 0.6 V, 0.7 V, and 0.8 V. The maximum current density sharply increased up to 1 M and then slightly increased until 5 M. It can be concluded that the Ni/Pd-decorated carbon nanofiber has a high performance for methanol electrooxidation up to 5 mol/L.

Figure 10 displays the chronoamperometric curve of the prepared Ni/Pd-doped carbon NFs in alkaline

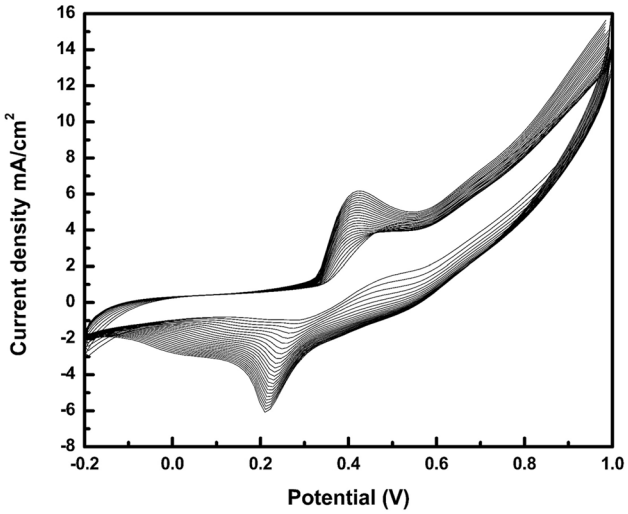

Fig. 8. Cyclic voltammetry results for the introduced Ni/Pd-doped CNF electrode in presence of methanol-free 1 M KOH solution at 25°C versus Ag/AgCl reference electrode; scan rate 100 mV/s.

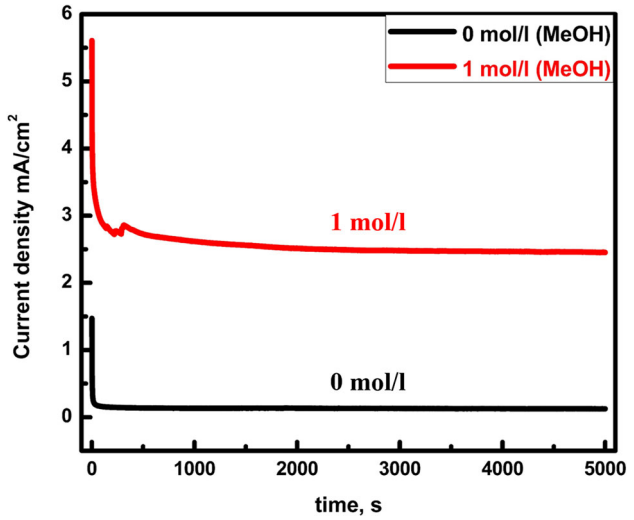

Fig. 10. Chronoamperometric analysis results for the introduced nanofibers in methanol-free 1.0 M KOH and after addition 1.0 M methanol at 0.4 V using Ag/AgCl as a reference electrode.

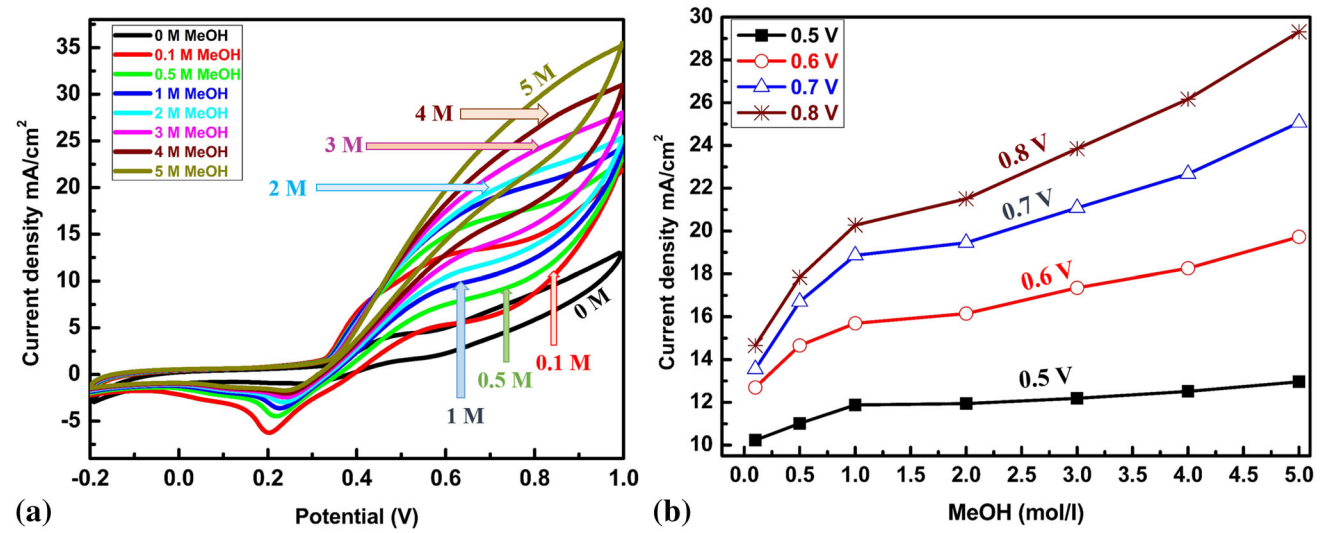

Fig. 9. The cyclic voltammograms of the Ni/Pd-doped CNFs using Ag/AgCl as a reference electrode at a scan rate of 50 mV/s and 25°C and different methanol concentrations, 0.1 mol/L, 0.5 mol/L, 1 mol/L, 2 mol/L, 3 mol/L, 4 mol/L, 5 mol/L (a), and effect of methanol on the maximum current density (b).

media. At short testing time, the current density decays from 5.608 mA/cm^2 to 3.410 after only 20 s. After 20 s, the rate of current gradually decreases and remains constant. Also, there is a big difference between the curve obtained in the case of 1 mol/L methanol and methanol-free. This difference can be due to the oxidation of methanol, which confirms the results obtained by Figs. 7 and 9. This long-term current stability is due to the formation of Ni&Pd—decorated by carbon NFs.[23,30,42]

Figure 11 displays the effect of scan rate on the behavior of methanol electrooxidation in 1 mol/L methanol at the same conditions. Two observations can be seen from the figure. The first is increasing of the area of voltammogram in low potential. Secondly, the current density grows at high potential. To conclude, the rate controlling step in electrooxidation of methanol has a diffusion character. At last, Table I shows a comparison between some Pt-free NFs, which were recently introduced to technology of direct methanol fuel cells. From this table, it is easy to deduce that Ni/Pd-carbon NFs can be used as an efficient anode catalyst for direct methanol fuel cells.

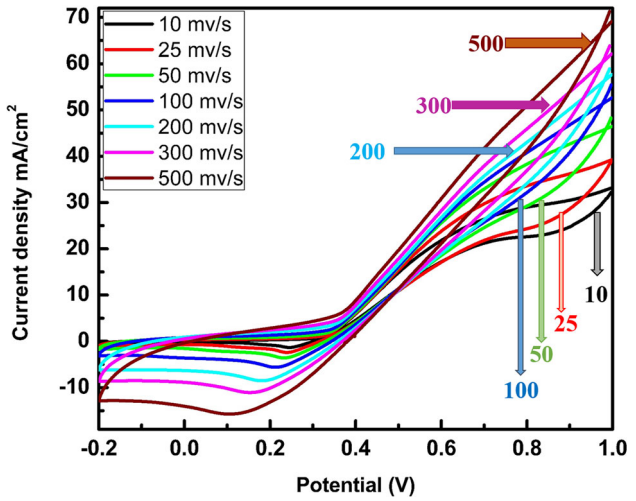

Fig. 11. Effect of scan rate on the electroactivity of the investigated catalyst in 1.0 M KOH containing 1.0 M methanol at 25°C using Ag/AgCl as a reference electrode.

CONCLUSION

In summary, the Ni/Pd nanoparticles incorporated carbon NFs have been successfully designed by a cheap methodology: electrospinning. The morphology, crystallinity, and chemistry of the designed material were investigated by SEM, XRD, FESEM, and TEM analysis including chemical mapping and EDX studies. Experimentally, the prepared NFs exhibit a high efficiency for methanol electrooxidation in alkaline medium up to 5 M. The current density improved in the presence of methanol from 4.17 mA/cm^2 (at 0 M MeOH) to 11.31 mA/cm^2 (at 1 M MeOH) at the same potential and temperature: 0.48 V and 25°C. This performance can be attributed to the combination between two electroactive elements, Ni and Pd in one-dimensional carbon nanostructure, which can enhance both catalytic process and electron transfer. From this point of view, this study opens a new area for development of non-precious one-dimensional nanostructure as a working electrode for direct methanol fuel cells.

Table I. Comparison of the activity of recent reported non-precious electrocatalysts @CNFs toward methanol oxidation in alkaline media at 0.4 V (the values extracted from the figures)

Catalyst	MeOH conc. (M)	Current density (mA/cm^2)	References
Co/CeO_2@CNFs	1	1.48	43
	3	2.37	
ZnO(40%)CeO_2 (60%) @CNFs	1	1.69	44
ZnO(60%)CeO_2 (40%) @CNFs	1	1.35	
Co/$SrCO_3$ nanorods @CNFs	1	2.19	45
Ni/Pd @CNFs	1	7.15	This work
Co-N@ CNFs	3	8.22	46
Co/Cu @CNFs	2	1.89	42
Co NPs		>0.1	
Cu NPs		>0.1	

ACKNOWLEDGEMENTS

This research was financially supported by National Research Foundation of Korea (NRF). Grant funded by the Korean Government (MOE) (No. 2014R1A1A2058967). The authors extend their appreciation to International Scientific Collaboration Program ISPP at King Saud University for funding this research work through ISPP-002.

CONFLICT OF INTEREST

The authors declare that there is no conflict of interests with other researchers.

REFERENCES

1. J. Chang, L. Feng, C. Liu, W. Xing, and X. Hu, *Energy Environ. Sci.* 7, 1628 (2014).
2. D. Aili, A. Vassiliev, J.O. Jensen, T.J. Schmidt, and Q. Li, *J. Power Sources* 279, 517 (2015).
3. B. Choi, W.-H. Nam, D.Y. Chung, I.-S. Park, S.J. Yoo, J.C. Song, and Y.-E. Sung, *Electrochim. Acta* 164, 235 (2015).
4. Z.L. Zhao, L.Y. Zhang, S.J. Bao, and C.M. Li, *Appl. Catal. B* 174, 361 (2015).
5. N.S. Veizaga, V.I. Rodriguez, T.A. Rocha, M. Bruno, O.A. Scelza, S.R. de Miguel, and E.R. Gonzalez, *J. Electrochem. Soc.* 162, F243 (2015).
6. H.D. Jang, S.K. Kim, H. Chang, J.-H. Choi, B.-G. Cho, E.H. Jo, J.-W. Choi, and J. Huang, *Carbon* 93, 869 (2015).
7. X. Zhao, M. Yin, L. Ma, L. Liang, C. Liu, J. Liao, T. Lu, and W. Xing, *Energy Environ. Sci.* 4, 2736 (2011).
8. Y.H. Chu and Y.G. Shul, *Int. J. Hydrog. Energy* 35, 11261 (2010).
9. A.A. Ensafi, M. Jafari-Asl, B. Rezaei, M.M. Abarghoui, and H. Farrokhpour, *J. Power Sources* 282, 452 (2015).
10. L. Zhang, Z. Wang, J. Zhang, X. Sui, L. Zhao, and J. Han, *Fuel Cells* 15, 619 (2015).
11. I.A. Raj and K. Vasu, *J. Appl. Electrochem.* 20, 32 (1990).
12. E. Akgül, A. Gülce, and H. Gülce, *J. Electroanal. Chem.* 668, 73 (2012).
13. I.M. Mohamed, V.-D. Dao, N.A. Barakat, A.S. Yasin, A. Yousef, and H.-S. Choi, *J. Colloid Interface Sci.* 476, 9 (2016).
14. I.M. Mohamed, V.-D. Dao, A.S. Yasin, H.M. Mousa, H.O. Mohamed, H.-S. Choi, M.K. Hassan, and N.A. Barakat, *Chem. Eng. J.* 304, 48 (2016).
15. Z.-M. Huang, Y.-Z. Zhang, M. Kotaki, and S. Ramakrishna, *Compos. Sci. Technol.* 63, 2223 (2003).
16. I.M. Mohamed, M. Motlak, M.S. Akhtar, A.S. Yasin, M.H. El-Newehy, S.S. Al-Deyab, and N.A. Barakat, *Ceram. Int.* 42, 146 (2016).
17. I.M. Mohamed, V.-D. Dao, A.S. Yasin, H.-S. Choi, and N.A. Barakat, *Int. J. Hydrog. Energy* 41, 10578 (2016).
18. H. He, L. Shi, Y. Fang, X. Li, Q. Song, and L. Zhi, *Small* 10, 4671 (2014).
19. M. Li, L. Liu, Y. Xiong, X. Liu, A. Nsabimana, X. Bo, and L. Guo, *Sensor. Actuators B chem.* 207, 614 (2015).
20. Q. Dong, G. Wang, B. Qian, C. Hu, Y. Wang, and J. Qiu, *Electrochim. Acta* 137, 388 (2014).
21. G. Zheng, Y. Yang, J.J. Cha, S.S. Hong, and Y. Cui, *Nano Lett.* 11, 4462 (2011).
22. A. Zainoodin, S. Kamarudin, M. Masdar, W. Daud, A. Mohamad, and J. Sahari, *Appl. Energy* 113, 946 (2014).
23. I.M. Mohamed, M. Motlak, H. Fouad, and N.A. Barakat, *NANO* 11, 1650049 (2016).
24. N.A. Barakat, M.A. Kanjwal, F.A. Sheikh, and H.Y. Kim, *Polymer* 50, 4389 (2009).
25. R. Amin, R.A. Hameed, K. El-Khatib, M.E. Youssef, and A. Elzatahry, *Electrochim. Acta* 59, 499 (2012).
26. C.-H. Cui, H.-H. Li, and S.-H. Yu, *Chem. Sci.* 2, 1611 (2011).
27. B.M. Thamer, M.H. El-Newehy, N.A. Barakat, M.A. Abdelkareem, S.S. Al-Deyab, and H.Y. Kim, *Electrochim. Acta* 142, 228 (2014).
28. S. Ha, R. Larsen, and R. Masel, *J. Power Sources* 144, 28 (2005).
29. A.S. Yasin, H.O. Mohamed, I.M. Mohamed, H.M. Mousa, and N.A. Barakat, *Sep. Purif. Technol.* 171, 34 (2016).
30. N.A. Barakat, M.A. Abdelkareem, A. Yousef, S.S. Al-Deyab, M. El-Newehy, and H.Y. Kim, *Int. J. Hydrog. Energy* 38, 3387 (2013).
31. Y. Zhao, X. Yang, J. Tian, F. Wang, and L. Zhan, *Int. J. Hydrog. Energ* 35, 3249 (2010).
32. N.A. Barakat, B. Kim, and H.Y. Kim, *J. Phys. Chem. C* 113, 531 (2008).
33. A. Yousef, M.S. Akhtar, N.A. Barakat, M. Motlak, O.-B. Yang, and H.Y. Kim, *Electrochim. Acta* 102, 142 (2013).
34. N.A. Barakat, M.S. Akhtar, A. Yousef, M. El-Newehy, and H.Y. Kim, *Chem. Eng. J.* 211, 9 (2012).
35. I. Danaee, M. Jafarian, A. Mirzapoor, F. Gobal, and M. Mahjani, *Electrochim. Acta* 55, 2093 (2010).
36. M. Simões, S. Baranton, and C. Coutanceau, *Appl. Catal. B* 93, 354 (2010).
37. C. Xu, H. Wang, P.K. Shen, and S.P. Jiang, *Adv. Mater.* 19, 4256 (2007).
38. A. Rahim and R. Abdel, Hameed, and M. Khalil. *J. Power Sources* 134, 160 (2004).
39. M. Vuković, *J. Appl. Electrochem.* 24, 878 (1994).
40. O. Enea, *Electrochim. Acta* 35, 375 (1990).
41. J. Liu, T. Zhao, R. Chen, and C. Wong, *Electrochem. Commun.* 7, 288 (2005).
42. N.A. Barakat, M. El-Newehy, S.S. Al-Deyab, and H.Y. Kim, *Nanoscale Res. Lett.* 9, 1 (2014).
43. Z.K. Ghouri, N.A. Barakat, M. Obaid, J.H. Lee, and H.Y. Kim, *Ceram. Int.* 41, 2271 (2015).
44. Z.K. Ghouri, N.A. Barakat, H.Y. Kim, M. Park, K.A. Khalil, M.H. El-Newehy, and S.S. Al-Deyab, *Arab. J. Chem.* 9, 219 (2016).
45. Z.K. Ghouri, N.A. Barakat, M. Park, B.-S. Kim, and H.Y. Kim, *Ceram. Int.* 41, 6575 (2015).
46. B.M. Thamer, M.H. El-Newehy, S.S. Al-Deyab, M.A. Abdelkareem, H.Y. Kim, and N.A. Barakat, *Appl. Catal. A* 498, 230 (2015).